Turkish Journal of Chemistry

http://journals.tubitak.gov.tr/chem/

Research Article

Turk J Chem
(2019) 43: 185 – 196
© TÜBİTAK
doi:10.3906/kim-1806-32

Crystal structure and Hirshfeld surface analysis of 1,2-ethylene-*bis* (*para*-methyl pyridinium) dichromate as a new selective and mild agent in oxidation of alcohols

Mostafa GHOLIZADEH[1,*], Mehrdad POURAYOUBI[1], Mohammad Reza HOUSAINDOKHT[1], Hadi AMIRI RUDBARI[2], Masoumeh FARIMANEH[1], Anahid SANEEI[1], Giuseppe BRUNO[3]

[1]Department of Chemistry, Faculty of Science, Ferdowsi University of Mashhad, Mashhad, Iran
[2]Faculty of Chemistry, University of Isfahan, Isfahan, Iran
[3]Department of Inorganic Chemistry, University of Messina, Messina, Italy

Received: 12.06.2018 • **Accepted/Published Online:** 09.11.2018 • **Final Version:** 05.02.2019

Abstract: 1,2-Ethylene-*bis*(*para*-methyl pyridinium) dichromate, $(C_{14}H_{18}N_2)[Cr_2O_7]$, is used as a new oxidizing agent in conversion of some alcohols to their corresponding carbonyl compounds in CH_3CN solvent and also under solvent-free conditions. In both procedures, high conversion percentages are observed. However, a much shorter reaction time is achieved in solvent-free conditions. For allylic alcohols, the C=C bond is not oxidized and the examined saturated alcohol in this work (i.e. *cyclo*-hexanol) remains intact, which illustrates the mild nature of reagent used. The structure of the reagent is investigated by single-crystal X-ray diffraction analysis. The C–H$\cdots$O and O$\cdots\pi$ interactions are the most important features of crystal packing, which are visualized by the Hirshfeld surface map.

Key words: Alcohol oxidation, 1,2-ethylene-*bis*(*para*-methyl pyridinium) dichromate, Hirshfeld surface analysis, solvent-free condition, X-ray crystallography

1. Introduction

The transformation of alcohols into corresponding carbonyl compounds has been studied in organic synthesis.[1,2] The Collins reagent ($[C_5H_5N]_2CrO_3$) is one of the well-known oxidizing agents for such a reaction.[3] To date, several efficient chromium(VI) reagents such as ammonium and pyridinium dichromates,[4–6] pyridinium chlorochromate,[7,8] 2,2-bipyridinium chlorochromate,[9] 2,6-dicarboxypyridinium fluorochromate,[10] 1-methylimidazolium chlorochromate,[11] and 1-(benzoylamino)-3-methylimidazolium chlorochromate[12] have been introduced to improve the selectivity, mildness, and effectiveness of the Cr^{VI}-based oxidant species in the oxidation of alcohols.

When the dichromate anion combines with an organic cation, it becomes a very useful agent for the oxidation of organic compounds in nonaqueous solutions[4–6] because the cation can control the oxidation properties and solubility of the reagent. It has been shown that the nature of amine-based cations determines the oxidizing power of the dichromate salts, which is inversely related to the donor strength of the amines.[13] The cation changes the pH value of the salt, which affects its oxidation property, as the electromotive force value of dichromate is strongly influenced by the concentration of H^+ (the half-cell of $Cr_2O_7^{2-}$ to $2Cr^{3+}$ needs $14H^+$).

*Correspondence: m_gholizadeh@um.ac.ir

Although many chromium(VI) reagents are available for the oxidation of organic substrates, there still exist certain limitations such as instability and poor selectivity toward the substrate(s), which calls for introducing new oxidants. Recently we developed the syntheses of some oxidizing agents, such as $(C_{12}H_{14}N_2)[Cr_2O_7]$[14] and $(C_{12}H_{14}N_2)[IO_3]_2$.[15]

Here we have synthesized a new dichromate-based oxidizing agent, $(C_{14}H_{18}N_2)[Cr_2O_7]$, as shown in the Scheme, and its performance in the oxidation process of various types of alcohols (benzylic, allylic, and saturated) was examined. The synthesized agent includes a bulk protecting organic dication with a low acidic characteristic, which leads to a selective oxidation property. The conversion percentage of an alcohol sample to its corresponding carbonyl compound was studied in solvent-free conditions in order to obtain the optimum temperature and molar ratio of reagent to substrate. The conversion was also examined in solution media, testing different solvents, and CH_3CN was found as the best solvent compared to the others used. Then the oxidation reactions of ten alcohols **were** performed in CH_3CN and also under solvent-free conditions for comparison.

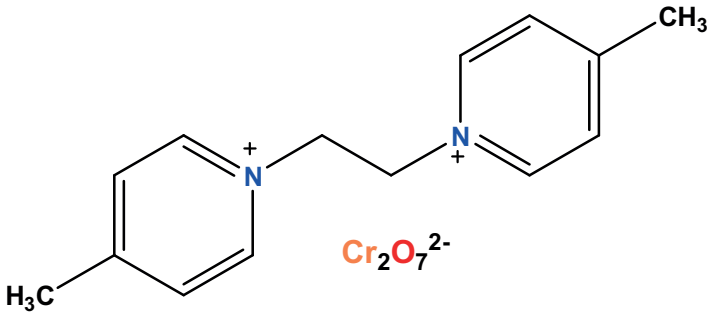

Scheme. New dichromate-based oxidizing agent, $(C_{14}H_{18}N_2)[Cr_2O_7]$.

The structure of the reagent was studied by single-crystal X-ray diffraction experiments, and the detailed investigation of intermolecular contacts was explored by Hirshfeld surface (HS) analysis and fingerprint plots.

2. Results and discussion

2.1. Oxidation of alcohols

The pH value of the title reagent (5.25, 0.01 M) confirmed its mild oxidizing nature. Typically, some examples of chromate salts with lower pH values and higher oxidizing abilities are as follows: $ZnCr_2O_7.3H_2O$ (2.85),[16] $Zn(ClCrO_3)_2.9H_2O$ (2.30),[17] and $(C_5H_5NH)(ClCrO_3)$ (1.75).[8] For investigating the ability of $(C_{14}H_{18}N_2)[Cr_2O_7]$ to oxidize alcohols, a solvent-free methodology was first studied on 4-chlorobenzyl alcohol in order to optimize the reaction conditions. The optimum temperature of 80 °C was obtained, with 0.5:1.0 molar ratio of oxidant and alcohol, as shown in Table 1. Finally, at this temperature, conversion is obtained at about 100% after a reaction time of 8 min.

The oxidation of 4-chlorobenzyl alcohol was then examined in different nonpolar and polar solvents, the results of which are listed in Table 2, and acetonitrile was found to be the best solvent medium.

After obtaining the optimum solvent medium, molar ratio, and temperature, some other alcohols were investigated in CH_3CN and also under solvent-free condition. The yields of carbonyl compounds in Table 3 were calculated by the weights of the related 2,4-dinitrophenylhydrazones. The reaction time in the solvent-free condition is less than that in CH_3CN.

Table 1. Oxidation of 4-chlorobenzyl alcohol using $(C_{14}H_{18}N_2)[Cr_2O_7]$ under solvent-free conditions.

Entries	Mol (oxidant:alcohol)	Temp (°C)	Time (min)	Conversion (%)
1	1.0:1.0	0	60	40
2	1.0:1.0	60	30	50
3	1.0:1.0	80	10	100
4	1.0:1.0	100	8	100
5	0.5:1.0	80	8	100
6	0.5:1.0	100	7	100

Table 2. Oxidation of 4-chlorobenzyl alcohol using $(C_{14}H_{18}N_2)[Cr_2O_7]$ in different solvents.

Entries	Solvent	Mol (oxidant: alcohol)	Time (h)	Yield (%) [a,b]
1	Water	1.0:1.0	24	30
2	CH_3CN	0.5:1.0	5	85
3	CH_3CN	1.0:1.0	2	85
4	CH_2Cl_2	1.0:1.0	24	20
5	Acetone	1.0:1.0	2	70
6	$CHCl_3$	1.0:1.0	24	50
7	n-Hexane	1.0:1.0	24	0
8	CH_3NO_2	1.0:1.0	24	20
9	t-BuOH	1.0:1.0	24	50
10	THF	1.0:1.0	24	0
11	1,4-Dioxane	1.0:1.0	5	80

[a]Yields at reflux temperature.

[b]Yields refer to 2,4-dinitro phenylhydrazone product.

Table 3. Oxidation of some alcohols using $(C_{14}H_{18}N_2)[Cr_2O_7]$ under different conditions.

Entries	Substrate	Product	Yield (%) [a](Time)	
			Solvent-free	Acetonitrile
1	$C_6H_5CH_2OH$	$C_6H_5C(O)H$	91 (10 min)	88 (150 min)
2	4-Cl-$C_6H_4CH_2OH$	4-Cl-$C_6H_4C(O)H$	94 (8 min)	85 (120 min)
3	2-Cl-$C_6H_4CH_2OH$	2-Cl-$C_6H_4C(O)H$	80 (30 min)	80 (300 min)
4	4-Br-$C_6H_4CH_2OH$	4-Br-$C_6H_4C(O)H$	87 (15 min)	90 (150 min)
5	2-NO_2-$C_6H_4CH_2OH$	2-NO_2-$C_6H_4C(O)H$	70 (40 min)	65 (420 min)
6	$C_6H_5CH(OH)CH_3$	$C_6H_5C(O)CH_3$	82 (35 min)	77 (330 min)
7	$C_6H_5CH(OH)C_6H_5$	$C_6H_5C(O)C_6H_5$	88 (25 min)	80 (210 min)
8	$C_6H_5CH{=}CHCH_2OH$	$C_6H_5CH{=}CHCHO$	70 (60 min)	65 (600 min)
9	$CH_2{=}CHCH_2OH$	$CH_2{=}CHCHO$	80 (20 min)	70 (330 min)
10	*Cyclo*-$C_6H_{11}OH$	*Cyclo*-$C_6H_{10}O$	N.R. (60 min)	N.R. (700 min)

[a]Yields refer to 2,4-dinitro phenylhydrazone products.

N.R. = No reaction.

For allylic alcohols, the C=C bond was not oxidized. The examined saturated alcohol (*cyclow* -hexanol) remained intact. Overoxidation of products to their corresponding carboxylic acids was not observed in any single case. Furthermore, during the reaction, functional groups such as chloro, bromo, and nitro were also insensitive to this reagent and also no byproduct was observed (Tables 1–3).

2.2. X-ray crystallography investigation

A search in the Cambridge Structural Database (CSD, Version 5.38, Feb 2017)[18] for dichromate anion indicates 57 different crystallographic structures for salts including organic cations, such as $(C_5H_6N)_2[Cr_2O_7]$[19] (CSD ref code: COXYAP02), $(C_{19}H_{18}P)_2[Cr_2O_7]$[20] (YUHLIW), $(C_5H_{14}N_3)_2[Cr_2O_7]$[21] (EQICOX), and $(C_{21}H_{46}N)_2[Cr_2O_7]$[22] (JIVQIO). Here we report the structure of $(C_{14}H_{18}N_2)[Cr_2O_7]$ salt. The crystallographic data and the details of the X-ray analysis are presented in Table 4 and selected bond lengths and angles are given in Table 5.

The asymmetric unit of the title compound contains one $(C_{14}H_{18}N_2)^{2+}$ dication and one $[Cr_2O_7]^{2-}$ dianion, as shown in Figure 1. In the dication, the two 4-methylpyridinium segments are in antiorientation with respect to each other, reflected in the N-C-C-N torsion angle of 179.4(4)°. In the dianion, the Cr(VI) centers are in a slightly distorted tetrahedral coordination environment. The oxygen atom of the Cr–O–Cr moiety and one of the terminal oxygen atoms are disordered over two sites with refined occupancies of 0.820(12):0.180(12) and 0.777(17):0.223(17), respectively.

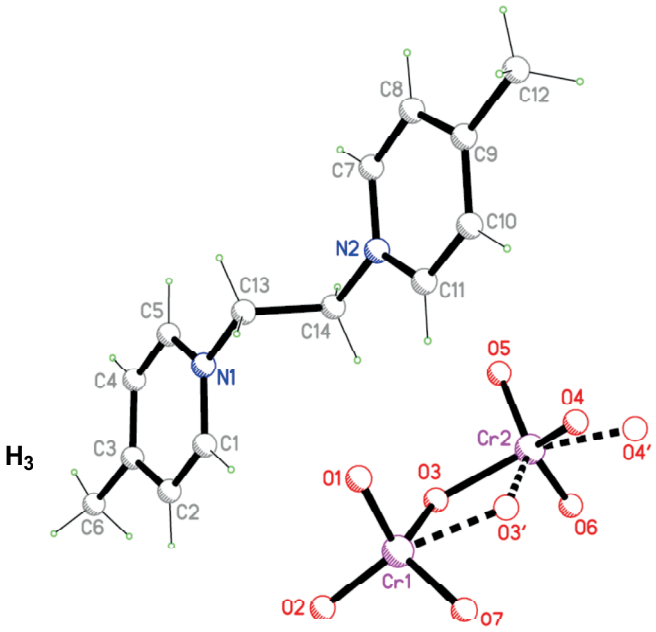

Figure 1. Molecular structure and atom labeling scheme for $(C_{14}H_{18}N_2)[Cr_2O_7]$. Dashed lines indicate the minor disorder component.

In the crystal packing, a $3D$ superstructure is built on the basis of the C-H$\cdots$O and O$\cdots\pi$ interactions. In this assembly, each dichromate anion receives hydrogen bonds from seven neighboring cations and each cation is surrounded by seven anions (Figure 2). The C-H$\cdots$O interactions occur between all of the seven oxygen atoms of the dianion and the CH units of the cation, except two CH units from two methyl groups, which do not take part in the hydrogen bonds. The details of H$\cdots$O distances are given in Figure 2.

Table 4. Crystallography data for $(C_{14}H_{18}N_2)[Cr_2O_7]$.

Formula	$C_{14}H_{18}Cr_2N_2O_7$
Mw	430.30
Temperature (K)	298(2)
Wavelength (Å)	0.71073
Crystal system	Orthorhombic
Space group	*Pbca*
a, Å	11.2480(3)
b, Å	14.3047(3)
c, Å	21.5127(5)
V, Å^3	3461.38(14)
Z	8
D_x	1.651 g cm^{-3}
Absorption coefficient, mm^{-1}	1.294
$F(000)$	1760
Crystal size, mm^3	0.26 × 0.18 × 0.12
θ range for data collection, deg.	2.49–26.00
Limiting indices	$-13 \leq h \leq 13$
	$-17 \leq k \leq 17$
	$-26 \leq l \leq 26$
Refl. collected / unique	136572 / 3402
R_{int}	0.0759
Completeness to θ (= 26.00°)	100.0%
Observed refls [$I \geq 2\sigma(I)$]	2286
Absorption correction	Full-matrix
Max. / min. transmission	0.6257 / 0.7456
Refinement method	Full-matrix least-squares on F^2
Data / restraints / parameters	3402 / 0 / 246
GoF (F^2)	1.132
Final R_1 / wR_2 [$I > 2\sigma(I)$]	0.0676 / 0.1599
R_1 / wR_2 (all data)	0.1047 / 0.1957
Largest diff. peak / hole, e Å^{-3}	0.701 / –0.466

The lone pair-π interactions were observed between the terminal O2 and O6 atoms with the N1/C1/C2/C3/C4/C5 and N2/C7/C8/C9/C10/C11 rings, respectively, with the separations of O2…Cg1 = 3.484 Å and O6…Cg2 = 3.005 Å (Cg1 and Cg2 are the centroids of the rings noted). More details of intermolecular interactions could be visualized using HS analysis (see below).

2.3. HS analysis

HS analysis is a new approach for graphical study of all contacts in a crystal and also for providing detailed quantitative information.[23,24] This method extends the study of intermolecular interactions to all of the contacts

Table 5. Selected bond lengths (Å) and bond angles (°) for $(C_{14}H_{18}N_2)[Cr_2O_7]$.

O3-Cr1	1.757(5)	O3-Cr2	1.809(5)
O3'-Cr2	1.72(3)	O3'-Cr1	1.90(4)
O4-Cr2	1.560(6)	O4'-Cr2	1.79(3)
O7-Cr1	1.537(6)	Cr1-O1	1.591(5)
C1-N1	1.342(8)	N1-C5	1.347(7)
N1-C13	1.486(7)	N2-C11	1.346(7)
N2-C7	1.352(7)	N2-C14	1.467(7)
Cr1-O3-Cr2	130.1(3)	O7-Cr1-O1	113.0(4)
O7-Cr1-O2	109.3(3)	O6-Cr2-O3	103.2(3)
C11-N2-C7	119.5(5)	C11-N2-C14	120.0(5)
C7-N2-C14	120.5(5)	C1-N1-C5	119.8(5)
C1-N1-C13	119.9(5)	C5-N1-C13	120.2(5)

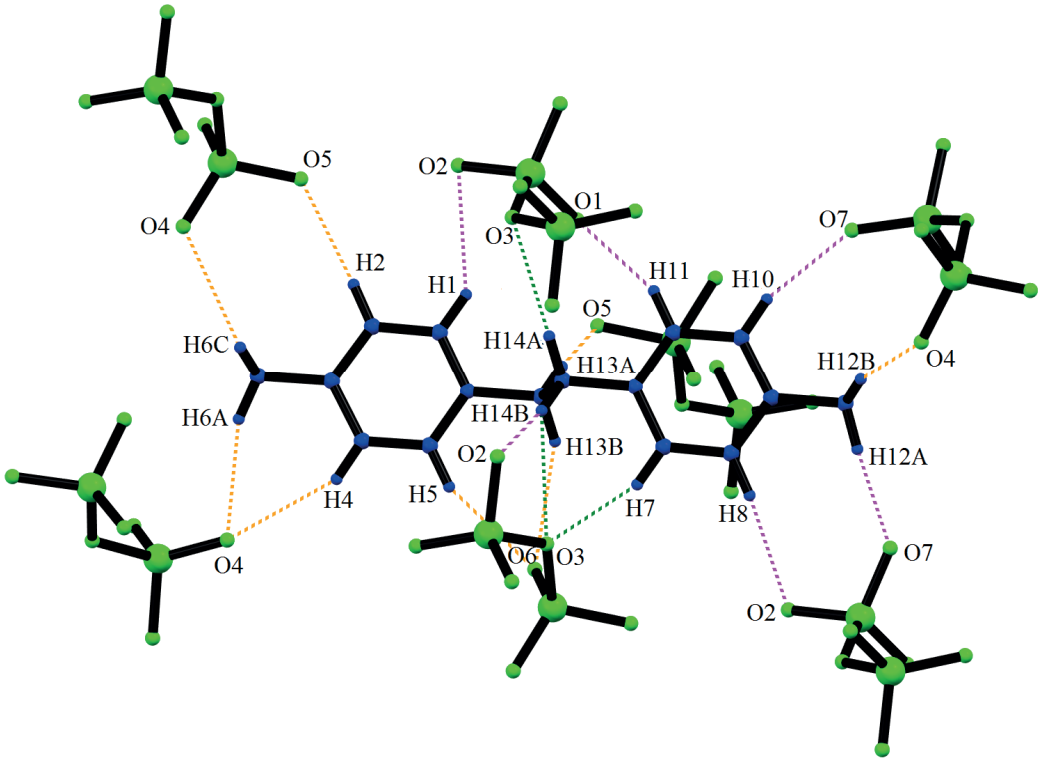

Figure 2. Crystal packing of $(C_{14}H_{18}N_2)[Cr_2O_7]$, showing cation hydrogen-bonded to neighboring anions through C-H$\cdots$O interactions. The minor disorder component was not shown for clarity. The magenta and orange dashed lines indicate the C-H$\cdots$O contacts with terminal O1/O2/O7 and O4/O5/O6 atoms, respectively. The green dashed lines show the C-H$\cdots$O contacts with bridge O3 atom. The H$\cdots$O distances are as follow: H7$\cdots$ O3 2.276 Å, H12A$\cdots$O7 2.306 Å, H10$\cdots$O7 2.342 Å, H13A$\cdots$O5 2.377 Å, H2$\cdots$O5 2.382 Å, H11$\cdots$O1 2.391 Å, H14B$\cdots$O2 2.419 Å, H8$\cdots$O2 2.435 Å, H5$\cdots$O6 2.438 Å, H4$\cdots$O4 2.580 Å, H13B$\cdots$O6 2.609 Å, H6A$\cdots$O4 2.624 Å, H12B$\cdots$O4 2.660 Å, H14A$\cdots$O3 2.664 Å, H6C$\cdots$O4 2.694 Å and H14B$\cdots$O3 2.701 Å.

in the structure, including the weak ones.[25] In a HS map, the red regions imply contacts shorter than van der Waals (vdW) radii, while the blue and white areas indicate contacts longer than and equal to the sum of vdW radii, respectively.[26]

In our study, the HS analysis was performed for the major disordered component. The results of the minor disordered component are very similar and are not discussed.

Front and back views of the HS maps of the cation and anion are shown in Figure 3 and the highlighted contacts (i.e. H$\cdots$O, H$\cdots$H, C$\cdots$O, and H$\cdots$Cr) are labeled in the maps and introduced in the caption of the figure. The "ball and stick" representation of the cation and anion has the same direction as the front view.

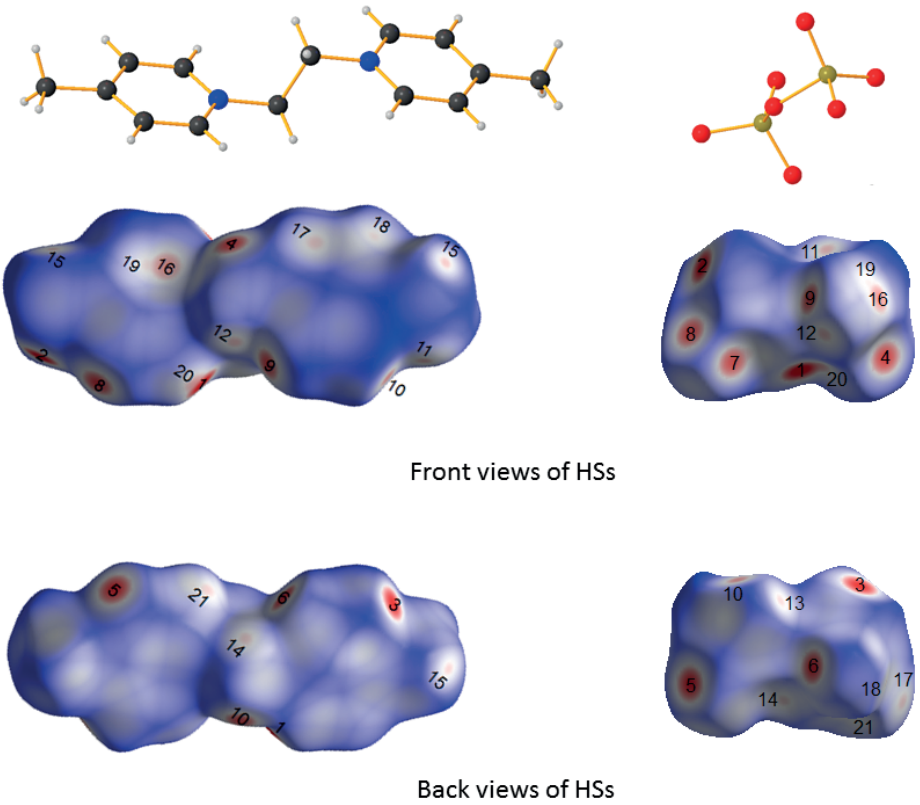

Figure 3. Front and back views of the Hirshfeld surfaces mapped with d_{norm}. Labels on HSs are as follows: C7-H7$\cdots$O3 (**1**), C12-H12A$\cdots$O7 (**2**), C10-H10$\cdots$O7 (**3**), C13-H13A$\cdots$O5 (**4**), C2-H2$\cdots$O5 (**5**), C11-H11$\cdots$O1 (**6**), C8-H8$\cdots$O2 (**7**), C5-H5$\cdots$O6 (**8**), C4-H4$\cdots$O4 (**9**), C14-H14B$\cdots$O2 (**10**), C6-H6A$\cdots$O4 (**11**), C13-H13B$\cdots$O6 (**12**), C12-H12B$\cdots$O4 (**13**), C14-H14A$\cdots$O3 (**14**), C6-H6B$\cdots$H12C-C12 (**15**), C11$\cdots$O6 (**16**), C1$\cdots$O2 (**17**), C2$\cdots$O1 (**18**), C10$\cdots$O6 (**19**), C7-H7$\cdots$Cr2 (**20**), and C1-H1$\cdots$Cr1 (**21**).

The lone pair$\cdots\pi$ interactions, discussed in the section on X-ray description, are shown in the HS map with the shape-index function, which illustrates the lone pair$\cdots\pi$ interactions quite conclusively (Figure 4).

2.4. Fingerprint plots

The fingerprint plots of cation and anion components are quite asymmetric, as shown in Figures 5 and 6. The asymmetry about the plot diagonal is typical of materials that contain more than one component in their crystal structures (molecule/ion), as interactions occur between two different species (cation and anion).[27]

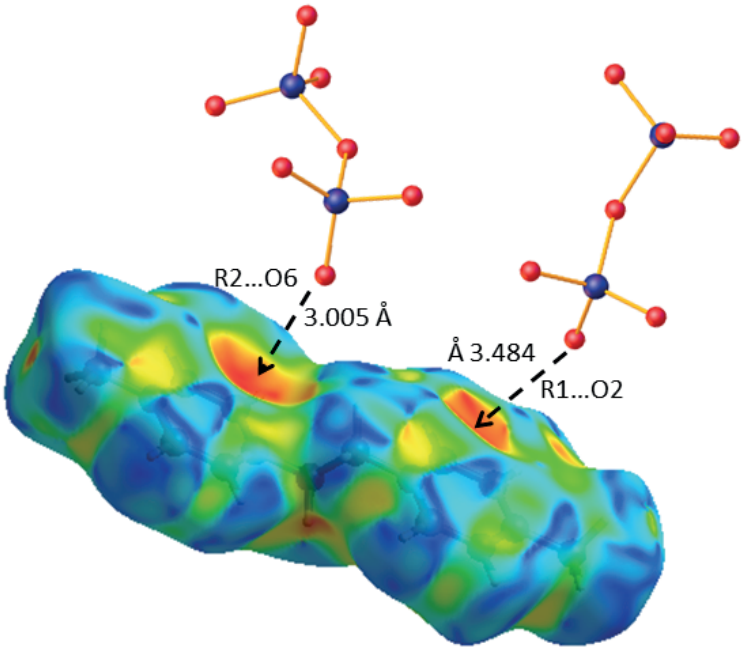

Figure 4. Hirshfeld surface mapped with the shape-index function, showing the lone pair...π interactions between O2 and O6 atoms with C1/C2/C3/C4/C5/N1 (named R1) and C7/C8/C9/C10/C11/N2 (R2) rings, respectively. The interacting anions are shown as a "ball and stick" model.

For the title structure, the divided 2D fingerprint plots of the cation and anion are given in Figures 5 and 6, respectively, which show the relative contribution proportion of contacts received by the component. For the cation in the title structure, the H$\cdots$O contacts constitute the highest proportion of interactions (41.9%) and develop as a sharp spike in the top left region of the plot ($d_e > d_i$). The H$\cdots$H contacts are the other main interactions in the cation (36.6%), followed by H$\cdots$C / C$\cdots$H, C$\cdots$O, and C$\cdots$C contacts that have a small share in the total interactions (Figure 5). For the anion, the O$\cdots$H contacts display the highest contribution proportion of interactions (90.0%) and the related points create one sharp spike in the related plot, with the shortest distance between donor and acceptor atoms (i.e. $d_i > d_e$) near 2.2 Å (Figure 6). The other interactions, i.e. O$\cdots$C, O$\cdots$O, and Cr$\cdots$H-C, have small contributions to the total interactions, with the percentages specified in Figure 5.

2.5. Conclusions

The synthesis, crystal structure, and intercomponent interactions of ethylene *bis*(*para*-methyl pyridinium) dichromate ($C_{14}H_{18}N_2$)[Cr_2O_7] oxidizing reagent were studied. It was found that the CH...O and O...π interactions are the most important features of crystal packing, which appears as red spots in the HS map (showing the contacts shorter than the sum of vdW radii).

The results revealed that this compound is an efficient reagent for the controlled oxidation of benzylic and allylic alcohols. The mild oxidation property of the reagent was proved on the basis of designed oxidation reactions as well as the pH value of the reagent in H_2O, without any evidence of side reactions or overoxidation. It was shown that the C=C bond in allylic alcohols is not oxidized and the examined saturated alcohol (*cyclo*-hexanol) remains intact, showing the mild nature of reagent used, due to its low acidic character.

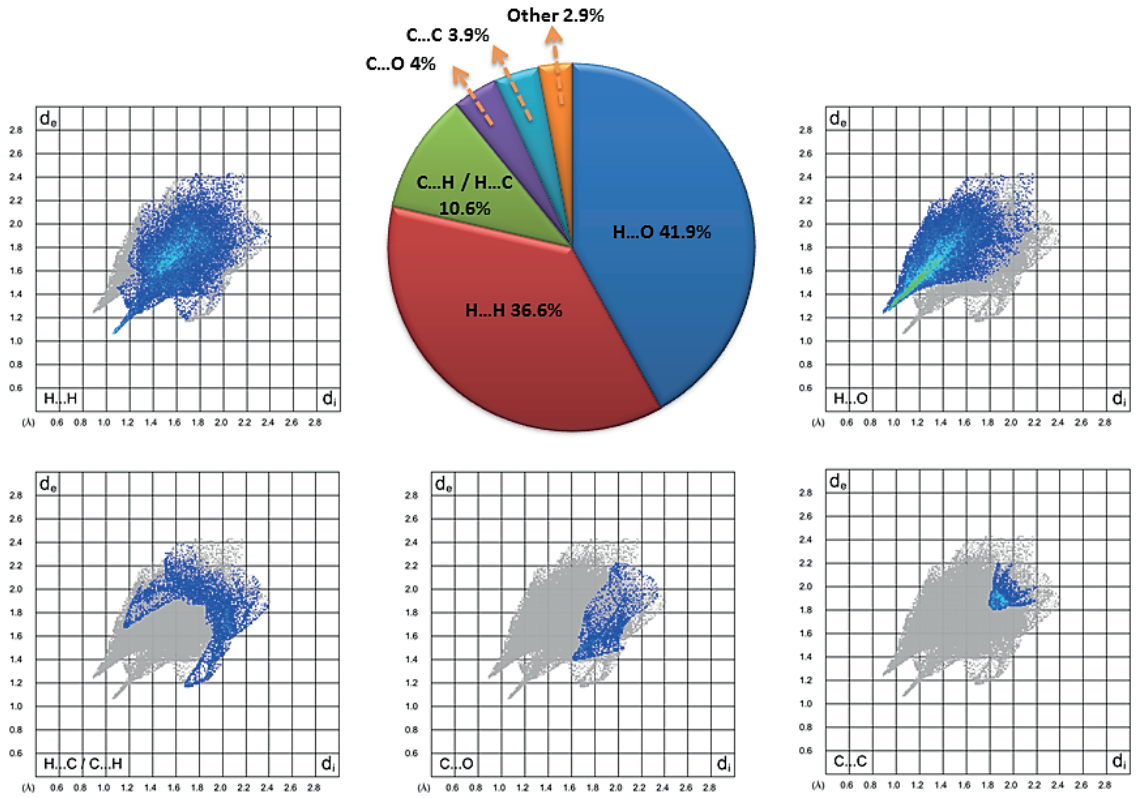

Figure 5. Decomposed 2D fingerprint plots of the cation, generated from the map given in Figure 3, left.

3. Experimental

3.1. Apparatus

The products were purified by column chromatography. The purity determination of the products was accomplished by TLC on silica gel Polygram STL G/UV 254 plates. The melting points of products were determined with an Electrothermal type 9100 melting point apparatus. The FT-IR spectra were recorded on an Avatar 370 FT-IR Thermo Nicolet spectrometer. The NMR spectra were provided by a Bruker Advance 100 MHz instrument. All of the products were well-known compounds and were characterized by the IR and ^{1}H NMR spectra and comparing their melting points with known compounds. Elemental analyses were performed using Elementar Vario EL III and Thermo Finnigan Flash EA 1112 Series instruments. The HSs and related fingerprint plots were generated by the Crystal Explorer 3.1 program.[28]

3.2. Preparation of ethylene *bis*(*para*-methyl pyridinium) bromide, $(C_{14}H_{18}N_2)Br_2$

A mixture of para-methyl pyridine (44 mmol) and 1,2-dibromoethane (22 mmol) in DMF (25 mL) was refluxed for 2 h. After cooling, the white solid formed was filtered, washed with CH_2Cl_2, and dried under vacuum (in 80% yield). Mp: 232 °C. ^{1}H NMR (D_2O, 100 MHz): δ 2.70 (s, 6H, CH_3), 5.21 (s, 4H, CH_2CH_2), 7.90 (d, J = 6 Hz, 4H), 8.60 (d, J = 6 Hz, 4H).

3.3. Preparation of ethylene *bis*(*para*-methyl pyridinium) dichromate, $(C_{14}H_{18}N_2)[Cr_2O_7]$

To a solution of $(C_{14}H_{18}N_2)Br_2$ (5 mmol) in H_2O (25 mL), a solution of $K_2Cr_2O_7$ (5 mmol) in H_2O (25 mL) was added and stirred. After 1 h, the reaction mixture was cooled to 0 °C and the orange solid

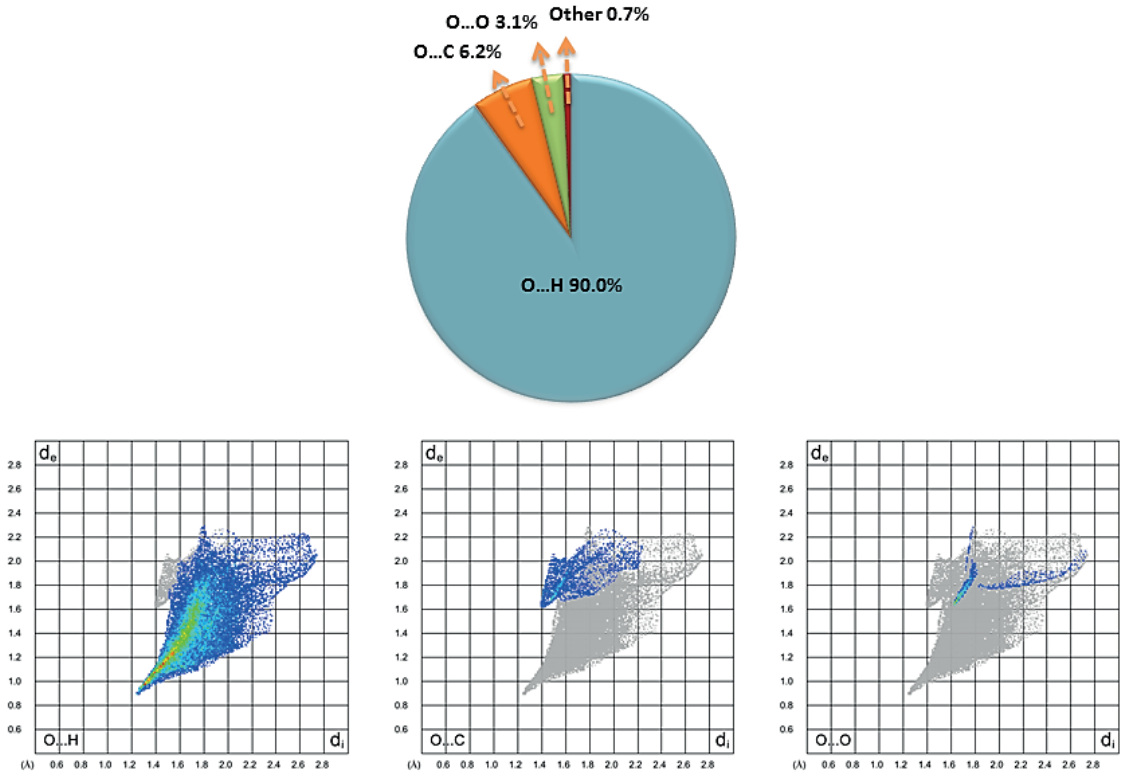

Figure 6. Decomposed 2D fingerprint plots of the anion component generated from the map given in Figure 3, right.

formed was collected by filtration, washed with cold water, and dried under vacuum (in 70% yield). The product was crystallized from H_2O/DMF (50:50) at room temperature. Mp: 153–155 °C. Anal. calcd. for $C_{14}H_{18}N_2Cr_2O_7$: C, 38.88; H, 4.02; N, 6.23. Found: C, 39.08; H, 4.22; N, 6.51.

3.4. General procedure for obtaining the optimum temperature, molar ratio, and time in the oxidation of alcohols under solvent-free conditions

A mixture of 4-chlorobenzyl alcohol and $(C_{14}H_{18}N_2)[Cr_2O_7]$ was stirred at the molar ratio, temperature, and time specified in Table 1. The crude oily/solid product was stirred in diethyl ether. The solvent was evaporated and the resulting crude material was purified by silica gel column chromatography. After optimization of temperature, molar ratio, and time, the reaction was performed between a mixture of an alcohol (1 mmol) and $(C_{14}H_{18}N_2)[Cr_2O_7]$ (0.5 mmol) at 80 °C for the time specified in Table 3. The crude oily/solid product was purified in the same way as noted for 4-chlorobenzyl alcohol.

3.5. General procedure for obtaining the best solvent medium and for oxidation of alcohols in CH_3CN

The $(C_{14}H_{18}N_2)[Cr_2O_7]$ agent was added to a solution of 4-chlorobenzyl alcohol in the solvent (5 mL) and the reaction mixture was refluxed with the molar ratio, solvent, and time specified in Table 2. The solvent was evaporated and diethyl ether was added to the residue. The supernatant was decanted and the insoluble residue was washed three times with diethyl ether. The combined ether extracts were concentrated under reduced

pressure and the crude product was purified by distillation or by passing through a short column of silica gel. After finding the best solution medium, CH_3CN, the reaction was performed for a mixture of an alcohol (1 mmol) and $(C_{14}H_{18}N_2)[Cr_2O_7]$ (1 mmol) in CH_3CN (5 mL) under reflux condition for the time given in Table 3. The crude oily/solid product was purified in the same way as noted for 4-chlorobenzyl alcohol.

3.6. X-ray structure determination

Single-crystal X-ray diffraction data for $(C_{14}H_{18}N_2)[Cr_2O_7]$ were collected on a Bruker APEX II equipped with a CCD area detector with Mo-Kα radiation (λ = 0.71073 Å) at room temperature. Data were collected and reduced by SMART and SAINT software in the Bruker packages.[29] The structure was solved by direct methods[30] and refined by least squares method on F^2.[31,32] All hydrogen atoms were placed in calculated positions and refined as isotropic with the "riding-model" technique.

3.7. Supplementary data

CCDC 908600 contains the supplementary crystallographic data for this paper. These data can be obtained free of charge from the Cambridge Crystallographic Data Centre via www.ccdc.cam.ac.uk/data_request/cif.

Acknowledgment

The authors are grateful for partial support of this work (Grant Number 3/22857) by Ferdowsi University of Mashhad Research Council.

References

1. Tojo, G.; Fernández, M. L. *Oxidation of Alcohols to Aldehydes and Ketones*; Springer: Berlin, Germany, 2006.
2. Sheldon, A.; Kochi, J. K. *Metal Catalysed Oxidations of Organic Compounds*; Academic Press: London, UK, 1981.
3. Collins, J. C.; Hess, W. W.; Frank, F. J. *Tetrahedron Lett.* **1968**, *9*, 3363-3366.
4. Corey, E. J.; Schmidt, G. *Tetrahedron Lett.* **1979**, *20*, 399-402.
5. Shirini, F.; Zolfigol, M. A.; Khaleghi, M. *Bull. Korean Chem. Soc.* **2003**, *24*, 1021-1022.
6. Sabita, P.; Mishra, B. K. *Tetrahedron* **2007**, *63*, 4367-4406.
7. Yilmaz, Ö.; Bekfelavi, E. Y.; Kuş, N. Ş.; Tunç, T.; Şahin, E. *Chem. Pap.* **2017**, *71*, 929-938.
8. Corey, E. J.; Suggs, J. W. *Tetrahedron Lett.* **1975**, *16*, 2647-2650.
9. Guziec, F. S. Jr.; Luzzio, F. A. *Synthesis* **1980**, 691-694.
10. Tajbakhsh, M.; Hosseinzadeh, R.; Sadatshahabi, M. *Synth. Commun.* **2005**, *35*, 1547-1554.
11. Kim, S.; Chang, H. *Bull. Korean Chem. Soc.* **1987**, *8*, 183-184.
12. Martinez, Y.; de las Heras, M. A.; Vaquero, J. J.; Garcia-Navio, J. L.; Alvarez-Builia, J. *Tetrahedron Lett.* **1995**, *36*, 8513-8516.
13. Guerrero, A. F.; Kim, H. J.; Schlecht, M. F. *Tetrahedron* **1988**, *29*, 6707-6709.
14. Gholizadeh, M.; Pourayoubi, M.; Kia, M.; Rheingold, A. L.; Golen, J. A. *Acta Cryst. E* **2012**, *68*, m305.
15. Gholizadeh, M.; Maleki, B.; Pourayoubi, M.; Kia, M.; Notash, B. *Acta Cryst. E* **2011**, *67*, o1614-o1615.
16. Firouzabadi, H.; Sardarian, A. R.; Moosavipour, H.; Afshari, G. R. *Synthesis* **1986**, *1986*, 285-288.
17. Firouzabadi, H.; Sharifi, A.; Karimi, B. *Iran. J. Chem. Chem. Eng.* **1993**, *12*, 32-35.

18. Groom, C. R.; Bruno, I. J.; Lightfoot, M. P.; Ward, S. C. *Acta Cryst. B* **2016**, *72*, 171-179.
19. Lennartson, A.; Håkansson, M. *Acta Cryst. C* **2009**, *65*, m182-m184.
20. Lorenzo, S.; Craig, D. C.; Scudder, M. L.; Dance, I. G. *Polyhedron* **1999**, *18*, 3181-3185.
21. Due-Hansen, J.; Stahl, K.; Boghosian, S.; Riisager, A.; Fehrmann, R. *Polyhedron* **2011**, *30*, 785-789.
22. Fosse, N.; Caldes, M.; Joubert, O.; Ganne, M.; Brohan, L. *J. Solid State Chem.* **1998**, *139*, 310-320.
23. McKinnon, J. J.; Spackman, M. A.; Mitchell, A. S. *Acta Cryst. B* **2004**, *60*, 627-668.
24. Spackman, M. A.; McKinnon, J. J. *CrystEngComm* **2002**, *4*, 378-392.
25. Saneei, A.; Pourayoubi, M.; Jenny, T. A.; Crochet, A.; Fromm, K. M.; Shchegravina, E. S. *Chem. Pap.* **2017**, *71*, 1809-1823.
26. McKinnon, J. J.; Jayatilaka, D.; Spackman, M. A. *Chem. Commun.* **2007**, *37*, 3814-3816.
27. Alamdar, A. H.; Pourayoubi, M.; Saneei, A.; Dušek, M.; Kučeráková, M.; Henriques, M. S. *Acta Cryst. C* **2015**, *71*, 824-833.
28. Wolff, S. K.; Grimwood, D. J.; McKinnon, J. J.; Turner, M. J.; Jayatilaka, D.; Spackman, M. A. *CrystalExplorer (Version 3.1)*; University of Western Australia: Perth, Australia, 2012.
29. Bruker Inc. *Bruker SMART (Version 5.060) and SAINT (Version 6.02A)*; Bruker AXS Inc.: Madison, WI, USA, 1999.
30. Burla, M. C.; Caliandro, R.; Camalli, M.; Carrozzini, B.; Cascarano, G. L.; De Caro, L.; Giacovazzo, C.; Polidori, G.; Spagna, R. *J. Appl. Cryst.* **2005**, *38*, 381-388.
31. Sheldrick, G. M. *SHELXL97 Program for Crystal Structure Refinement*; University of Göttingen: Göttingen, Germany, 1997.
32. Bruker Inc. *SHELXTL (Version 5.10)*; Bruker AXS Inc.: Madison, WI, USA, 1998.